Initial Draft

Investigation of Wave Energy Converter Effects on Near-shore Wave Fields:

Model Generation, Validation and Evaluation - Kaneohe Bay, HI

Jesse Roberts*, Grace, Chang**, and Craig Jones**

*Sandia National Laboratories
**Sea Engineering Inc.

March 2012

Table of Contents

Introduction

Kaneohe Bay, located on the windward (northeastern) side of the island of Oahu, Hawaii, presently has a shallow water (30 m) wave energy test berth and is under consideration to develop up to two additional berths in deeper waters (60 m - 70 m) potentially making it the location of the first full scale wave energy test site (WETS) in the United States (Figure 1). One objective of the WETS is to provide a location that contains all necessary in-water and land-side infrastructure to support simple connection of up to three wave energy conversion (WEC) devices for testing purposes. To support the site-selection process, it is necessary to determine the anticipated incident wave climate on the study site, as well as the effects of the WEC on the propagation of waves into shore. As such, a numerical model was developed in order to better comprehend both the existing condition (i.e. no WEC device) wave conditions and those that may be present when a WEC device (or WEC array) is installed. Specific concerns include, but are not limited to, impacts of the WEC device(s) on the near-shore recreational surf climate as well as resultant shoreline erosion.

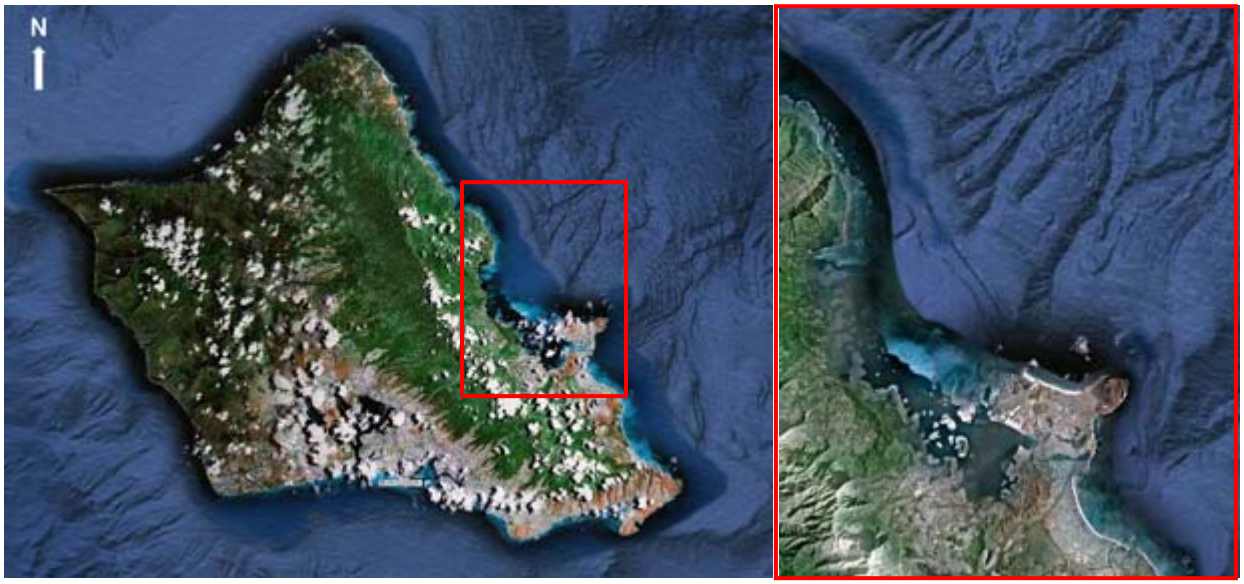

Figure 1. Left: Map of Oahu, HI with Kaneohe Bay outlined in red. Right: Map of Kaneohe Bay.

As deepwater waves approach the coast, they are transformed by certain processes including refraction (as they pass over changing bottom contours), diffraction (as they propagate around objects such as headlands), shoaling (as the depth decreases), and ultimately, energy dissipation (due to bottom friction and by breaking). The propagation of deepwater waves into the study site was modeled using the open-source program, SWAN (Simulating WAves Nearshore), developed by Delft Hydraulics Laboratory. SWAN has the capability of modeling all of the aforementioned processes in shallow coastal waters.

The SWAN model is a non-stationary (non-steady state) third generation wave model based on the discrete spectral action balance equation. SWAN is fully spectral over the total range of wave frequencies. Wave propagation is based on linear wave theory, including the effect of wave generated currents. The processes of wind generation, dissipation, and nonlinear wave-wave interactions are represented explicitly with state-of-the-science, third-generation formulations. SWAN provides many output quantities including, but not limited to, two dimensional spectra, significant wave height (H_s), wave period (mean and peak, T_p), wave direction (peak and mean, MWD), and directional spreading. The SWAN model has been successfully validated and verified in

laboratory and complex field cases. Sandia National Labs and Sea Engineering, Inc. (SEI) have validated the model at nearby Waimanalo Bay as well as several locations on the mainland United States (e.g. Santa Cruz Bight, Monterey Bay, and Humboldt Bay, California).

Model

The SWAN model requires minimum inputs typical of numerical wave propagation models: boundary conditions such as offshore deepwater wave parameters (H_s, T_p, and MWD) and the site's bathymetry. The digital elevation model (DEM) used to generate the model topography and bathymetry was gathered from an SEI survey of the proposed WETS location and the Main Hawaiian Islands Multibeam Synthesis project website, a part of the Hawaiian Mapping Research Group (HMRG) at the University of Hawaii at Manoa.[1]

Sea Engineering, Inc. has previously collected high-resolution multi-beam data within the proposed WETS boundaries. In addition, adjacent, high-resolution, near-shore multi-beam datasets and a coarse resolution (50 m grid spacing) dataset were obtained from the HMRG website to comprise sufficient data to fill the numerical modeling domain.

Figure 2 illustrates the SWAN model grid bathymetry and model domain extents. The bathymetric grid cell size is 50 meters on a side and the overall domain dimensions are roughly 25 km in the north-south direction and 30 km in the east-west direction. For model validation purposes, a simplistic, coarse grid model was employed. The coarse grid wave spectrum boundary conditions were parametrically specified along each of the offshore boundaries (northerly, easterly, and southerly) of the model domain in entirety. A constant parameter significant wave height, peak wave period, and mean wave direction was selected for each coarse grid modeling scenario and corresponding offshore wave spectra (frequency and direction) were subsequently generated by the model code. In order to investigate the potential effects of near-shore WEC devices, a nested grid model was operated such that the coarse grid model (described above) propagated waves from deepwater into a near-shore, finer grid model. Modeled wave spectra from the coarse grid were specified for each grid point in the finer grid model and allowed to propagate into shore.

The coarse grid offshore wave conditions for validation exercises were derived from National Oceanic and Atmospheric Administration (NOAA) National Data Buoy Center (NDBC) Station 51000. Westerly waves are blocked by land at Kaneohe Bay so only waves from a northerly and easterly direction were used as input to the model for validation. In this investigation, the model was run as a stationary (steady-state) model within SWAN. Model validation was provided with data from a near-shore Coastal Data Information Program (CDIP) buoy.

The coarse model computational grid comprised of the same overall domain dimensions as the grid bathymetry (25 km by 30 km). The computational grid spacing used for this investigation was 100 meters on a side. The coarser grid spacing provided for computationally efficient model generation, validation, and evaluation. In order to ascertain the local effects of small-scale WEC devices on the proximate wave conditions, a finer grid model computational grid was operated. The finer grid domain dimensions were approximately 1 km by 1 km with 20 meter grid spacing on a side (Figure 2).

[1] http:// www.soest.hawaiian.edu/HMRG/Multibeamn/index.php

WEC devices were represented in the model as "obstacles" to wave propagation. An obstacle, in model sense, hinders or completely blocks wave propagation. Though there are several options for specifying how obstacles are utilized in SWAN, the most basic is a specification of transmission and reflection coefficients, which basically specify the fraction of wave energy that is allowed to transmit past and the amount of wave energy that is reflected by, the obstacle. For simplicity and extreme conservatism, the transmission and reflection coefficients in this investigation were both set equal to 0 (i.e. no reflection or transmission, energy is 100% absorbed by the obstacle). These coefficient values will produce the largest changes in wave propagation parameters (e.g. wave heights and periods) and are considered environmentally conservative. More specific information on energy absorption will be incorporated in future work, when more information is known about the types of WEC devices that will be deployed at the WETS.

Furthermore, when obstacles are specified in SWAN, they need to intersect with a connection between two grid points to have any effect on model predictions. The implications of this are twofold: 1) Obstacle(s) may not have any effect on model predictions if they do not cross a grid point connection and 2) the effect of obstacles on wave propagation is directly dependent upon the computational grid spacing. Obstacles of varying dimensions may have the same effect on model predictions if they each cross the same connection(s) between grid points. In this model study, since the computational grid spacing is approximately 20 meters on a side, obstacles (i.e. WEC devices) smaller than this cannot be represented.

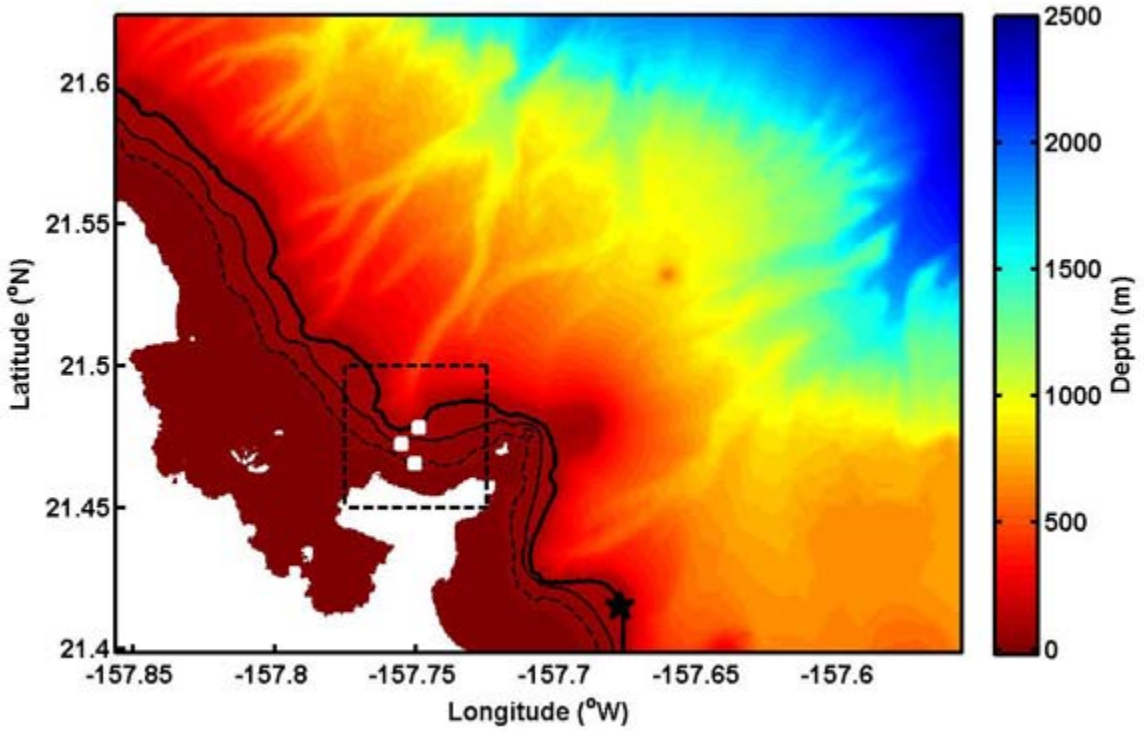

Figure 2. Model domain bathymetry with 30, 60, and 90 m contours drawn for reference. White coloring indicates land (elevation above 0 ft MSL). The dashed box denotes the boundaries of the finer grid, nested model. The black star indicates the location of the Mokapu Point CDIP buoy used for model validation. The white squares denote the locations of model obstacles to simulate WEC devices.

SWAN Validation

The SWAN model was validated by initiating coarse grid model scenarios with deepwater wave parameters obtained from the NOAA NDBC Station 51000[2]. The buoy is located at 23°32'47"N, 154°3'20"W in approximately 4000 meter water depth. Model results were extracted at coordinates 21°24.9'N, 157°40.70'W, which is the location of CDIP buoy Station 098, Mokapu Point[3]. The Mokapu Point CDIP buoy is located in approximately 100 m water depth.

To validate the model, significant wave heights, peak wave periods, and mean wave directions were extracted and compared to the measured data from CDIP Station 098. In this investigation, SWAN model validation was conducted for daily noon (1200 hours) and midnight (0000 hours), between 19 and 29 February 2012.

The ability of a wind-wave model to predict wave characteristics can be evaluated in many ways. Here, model performance analysis (model vs. measured) was assessed through the computation of root mean square error (RMSE), scatter index (SI), and bias (or mean error; ME). Scatter index is defined as the root mean square error normalized by the average observed (measured) value (Komen et al. 1994). Mean error allows for the detection and evaluation of bias in the wave characteristic data forecasts. When examining results of ME analysis, a positive value would indicate the average over-prediction of an observed value while a negative value indicates average under-prediction of the observed value. The model performance metrics are defined by the equations below.

$$RMSE = \sqrt{\frac{\sum_{i=1}^{N}(x_{1,i} - x_{2,i})^2}{N}}$$

$$SI = \frac{RMSE}{\bar{x}_{2,i}}$$

$$Bias = \frac{\sum_{i=1}^{N}(x_{1,i} - x_{2,i})}{N}$$

Where $x_{1,i}$ is model data, $x_{2,i}$ is measured data, N is the number of data points, and the over-bar in the equation for SI denotes the mean (arithmetic average) value.

The SWAN model performance statistics computed for the Mokapu Point location are presented in Table 1. Model data showed good agreement to observed data (Figure 3). The wave heights exhibited a mean error of 0.26 m (i.e. slight over-prediction). The peak periods showed a slight under-prediction of 0.21 s. The mean wave directions were over-predicted by approximately 15 degrees (clockwise) from the measured data. All values are considered within good agreement based on this limited validation period.

Table 1. SWAN model performance statistics computed for results at Mokapu Point.

Variable	RMSE	SI	Bias or ME
H_s (m)	0.40	0.14	0.26
T_p (s)	0.65	0.07	-0.21

[2] http://www.ndbc.noaa.gov
[3] http://cdip.ucsd.edu

MWD (°)	18.26	0.24	15.16

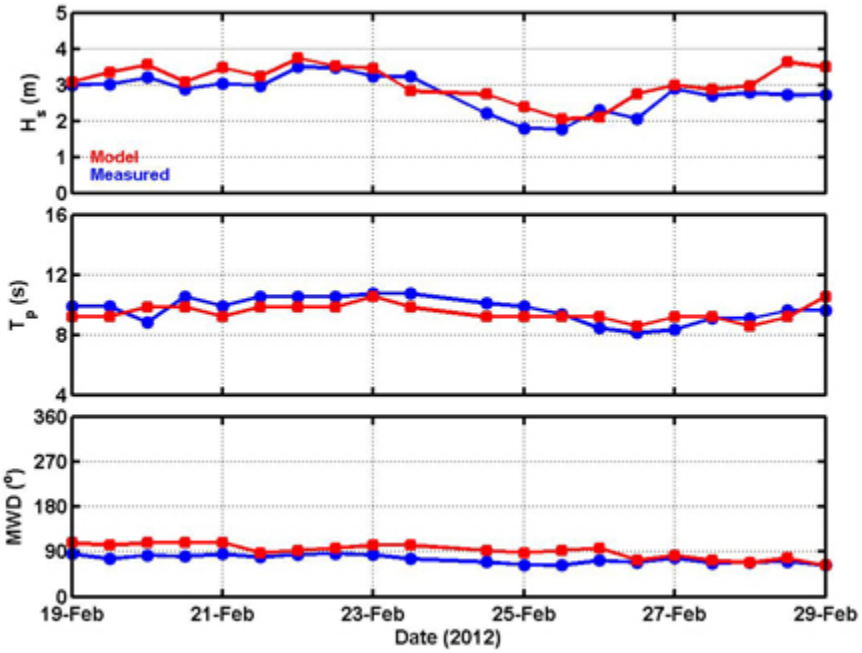

Figure 3. SWAN model validation results for Mokapu Point. Model data are shown in red and measured CDIP Station 098 data are shown in blue.

Uncertainty in these predictions may have arisen from multiple sources. The SWAN model is sensitive to bathymetry; therefore, the model is generally limited by the accuracy of the bathymetry available for a region. For the Kaneohe Bay SWAN model, available bathymetry resolution was high for near-shore locations, but was coarser offshore (50 meter grid spacing).

Additionally, offshore boundary conditions specified in the model validation were comprised of parameterized, constant significant wave height, peak period, and mean wave direction parameters; wave frequency and direction spectrum was generated from these parameters. Specification of offshore boundary conditions in this manner precluded the inclusion of wave spectra from multiple directions or multiple dominant frequencies (i.e. bi-modal wave spectra).

Results

Model utility was demonstrated by running the nested SWAN model for a sample range of typical wave conditions. Offshore, coarse grid (100 m grid spacing) boundary conditions comprised 1, 2, 3, and 4 m wave heights at peak periods of 6, 8, 10, 12, and 14 s and originating from mean wave directions of 0°, 30°, 60°, 90°, and 330°. The resulting coarse grid modeled wave spectra were then specified for each grid point in the finer grid model (20 m grid spacing) and allowed to propagate into shore.

The nested model was run with and without obstacles (WEC devices) to better comprehend both the existing condition (i.e. no WEC device) wave conditions and those that may be present when a WEC device (or WEC array) is installed. For model runs that included simulated WEC devices, an array of three obstacles was simulated (Figure 2). The location of the shallow water berth and the

approximate location of the two deeper water berths were provided by the Navy. Each obstacle was approximately 20 m in length (due to grid size constraints) and was located near WEC sites of interest (Table 2). Model obstacle reflection and transmission coefficients were set to 0.0 and 0.0, respectively. A total of 200 nested model runs were conducted (100 without obstacles and 100 with obstacles).

Table 2. Locations of the three obstacles for SWAN model runs.

Obstacle number	Latitude (°N)	Longitude (°W)	Depth (m)
1	21.4656	157.751	33
2	21.4726	157.755	52
3	21.4784	157.749	86

Figures 4 through 6 are examples of modeled significant wave height for nested SWAN runs with offshore boundary condition significant wave heights of 1, 2, 3, and 4 m and peak wave periods of 6 s (Figure 4), 10 s (Figure 5), and 14 s (Figure 6). Mean wave direction was held constant at 0° for these 12 model runs. Figures 7-10 illustrate model predictions with varying mean wave directions; the peak period was a constant (10 s) for the results shown in these images. The array of three obstacles was included in the SWAN model runs shown in Figure 4-10.

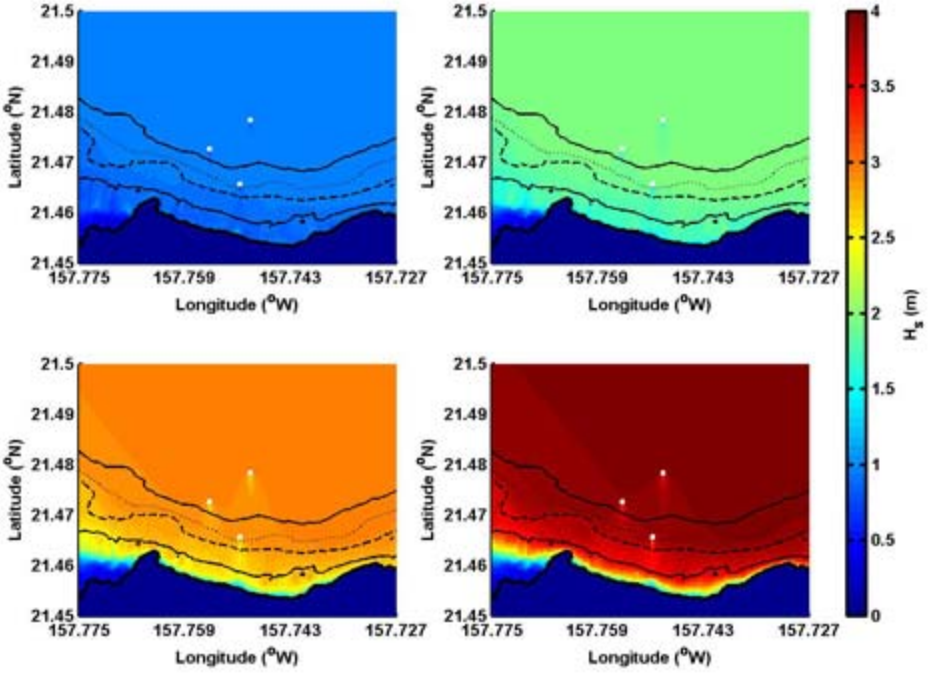

Figure 4. SWAN simulated significant wave height with model initiation parameters: MWD = 0°; T_p = 6 s; and H_s = 1 m (upper left), 2 m (upper right), 3 m (lower left), and 4 m (lower right). The bold line denotes the shoreline and contour lines for 10 m, 20 m, 30 m, and 40 m are shown. The model obstacles, shown as white squares, are not to scale.

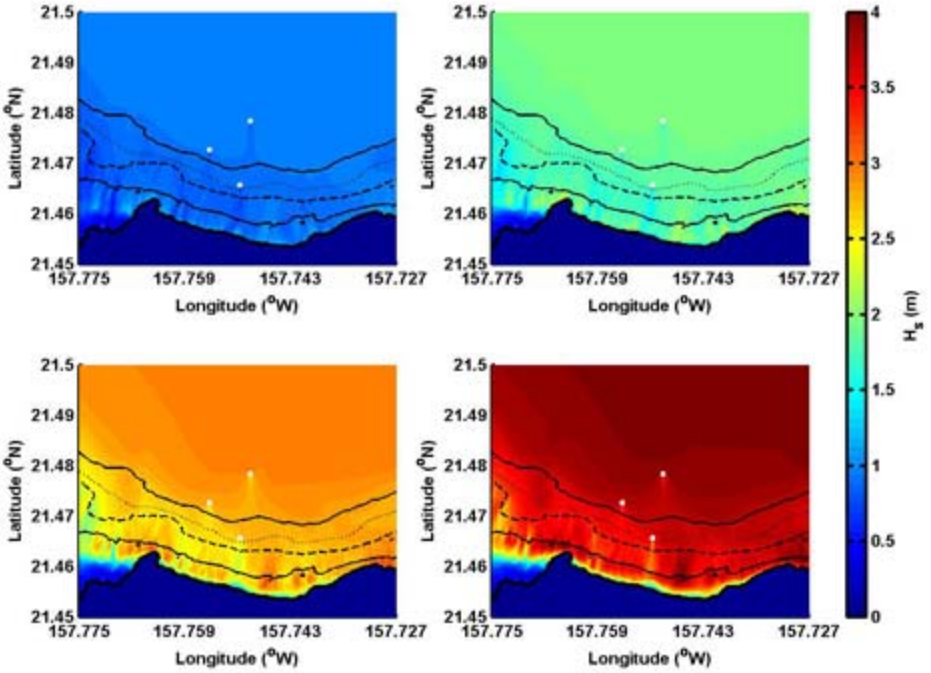

Figure 5. Same caption as Figure 4 but T_p = 10 s.

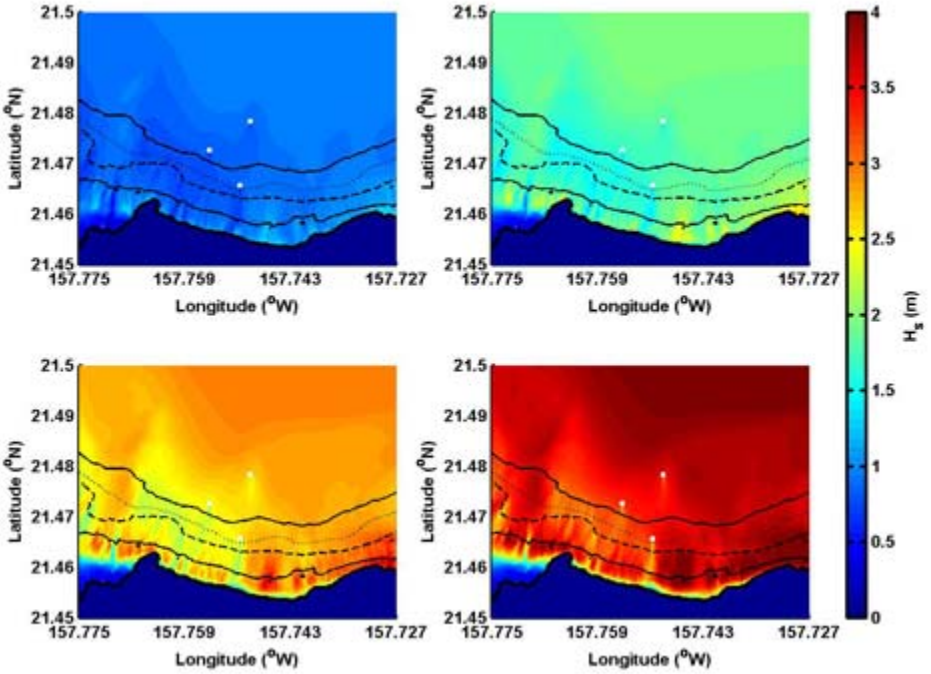

Figure 6. Same caption as Figure 4 but T_p = 14 s.

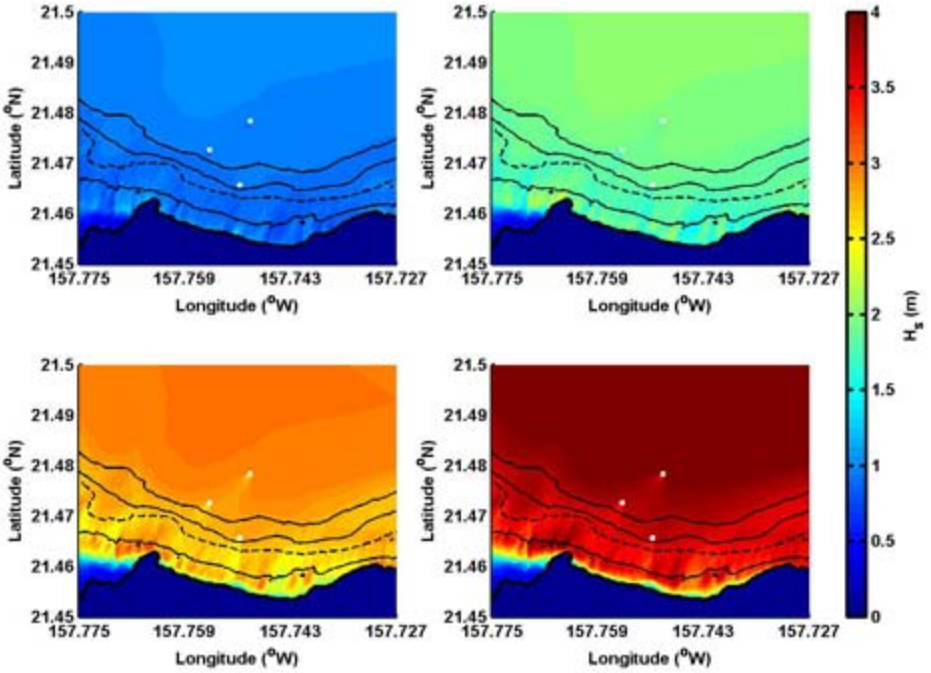

Figure 7. SWAN simulated significant wave height with model initiation parameters: MWD = 30°; T_p = 10 s; and H_s = 1 m (upper left), 2 m (upper right), 3 m (lower left), and 4 m (lower right).

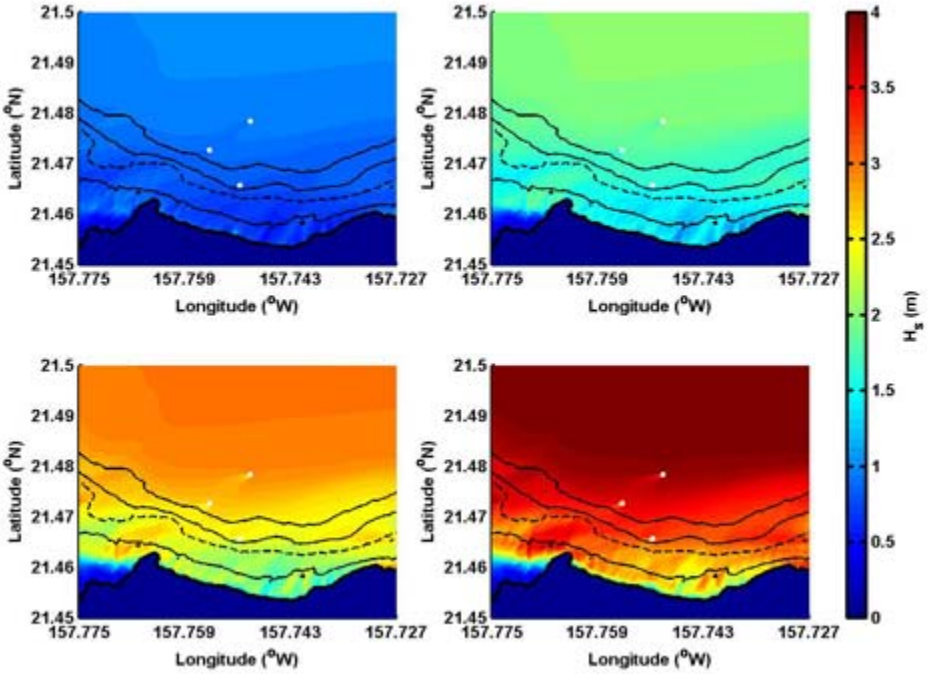

Figure 8. Same caption as Figure 7 but MWD = 60°.

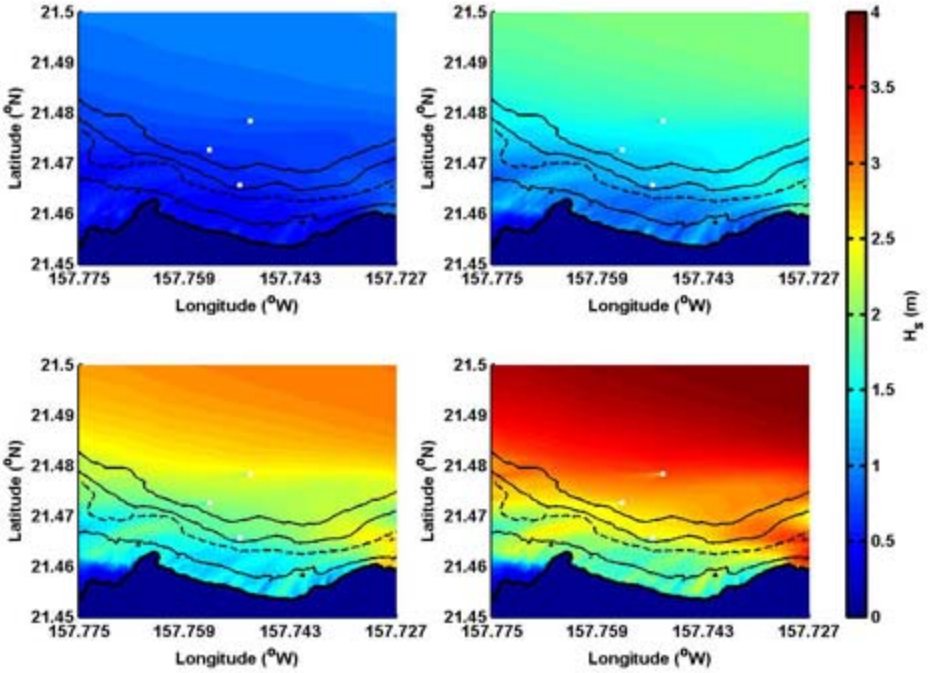

Figure 9. Same caption as Figure 7 but for MWD = 90°.

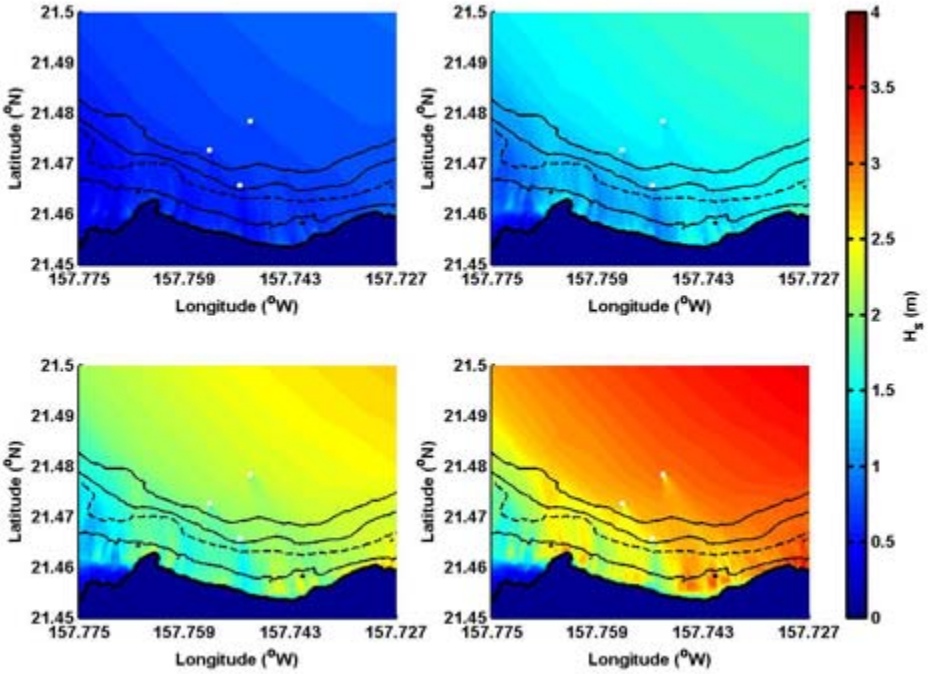

Figure 10. Same caption as Figure 7 but for MWD = 330°.

The effects of obstacle inclusion on the near-shore study area wave climate were evaluated by comparing model outputs *with* and *without* obstacles at nine (9) discrete model output locations (Table 3).

Table 3. Locations of nine (9) output points for evaluating effects of WEC devices (i.e. obstacles).

Output point #	Depth (m)*	Latitude (°N)	Longitude (°W)
1	20	21.4672	157.759
2	20	21.465	157.755
3	25	21.464	157.749
4	10	21.4638	157.76
5	10	21.46	157.755
6	10	21.459	157.749
7	5	21.461	157.761
8	5	21.458	157.755
9	5	21.456	157.749

*Approximate depth

On average, significant wave heights were 0.02 m smaller, or 1.4% less when obstacles were included in the modeling. In general, neither the water depth nor proximity to obstacles appeared to affect wave height differences with and without obstacles. The most obstacle impact variability (expressed as standard deviation; Table 4) was observed at output locations 6 and 9, which were the nearshore, easternmost locations and most affected by waves approaching from the east. Table 4 quantifies the general statistics at all model output locations. Percent differences were computed following:

$$\%\text{diff} = 100 * [(H_{s\,w/o} - H_{s\,w/})/H_{s\,w/o}].$$

Where $H_{s\,w/o}$ is modeled H_s without obstacles and $H_{s\,w/}$ is modeled H_s with obstacles.

Table 4. Statistics of the differences between H_s *with* and *without* obstacles at nine (9) output point locations for 100 nested model runs (model boundary conditions: H_s = 1, 2, 3, and 4 m; T_p = 6, 8, 10, 12, and 14 s, and MWD = 0, 30, 60, 90, and 330°). Values for the 5 m contour, 10 m contour, and 20-25 m contour are also provided.

Output location	Mean		Minimum		Maximum		Standard Deviation	
	%diff	m	%diff	m	%diff	m	%diff	m
1	1.08	0.023	0.01	0	2.69	0.097	0.95	0.026
2	2.01	0.037	0.94	0.009	4.03	0.114	0.82	0.023
3	0.68	0.013	0	0	3.41	0.099	0.95	0.019
4	1.20	0.024	0.02	0	2.62	0.094	0.80	0.023
5	2.0	0.038	0.19	0	3.11	0.098	0.74	0.025
6	1.65	0.029	0	0	6.32	0.148	2.23	0.040
7	1.10	0.017	0.01	0	2.35	0.056	0.74	0.014
8	1.50	0.025	0.04	0	3.11	0.069	0.91	0.017
9	1.26	0.018	0	0	5.96	0.104	1.94	0.028
5 m	1.29	0.020	0	0	5.96	0.104	1.19	0.020
10 m	1.62	0.030	0	0	6.32	0.148	1.26	0.029
20 – 25 m	1.26	0.024	0	0	4.03	0.114	0.91	0.023

Visual results for significant wave height differences (H_s *without* obstacles - H_s *with* obstacles) are shown in Figures 11-14.

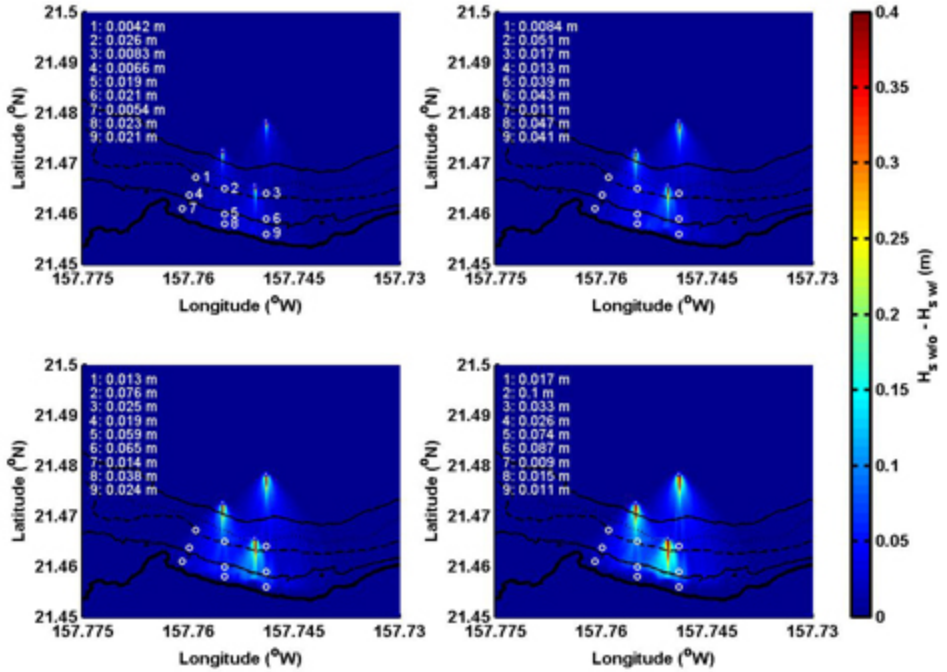

Figure 11. Evaluation of the effects of an obstacle array on the nearshore study area (obstacles – white squares – are not to scale). The model initiation parameters were: MWD = 0°; T_p = 10 *s*; and H_s = 1 m (upper left), 2 m (upper right), 3 m (lower left), and 4 m (lower right). The bold line denotes the shoreline and contour lines for 10 m, 20 m, 30 m, and 40 m are shown. Model output locations are indicated by white circles and are numbered in the upper left panel (see Table 3 for additional description). The differences between SWAN simulated significant wave height *without* and *with* obstacles for each output location are indicated on the left-hand side of each panel.

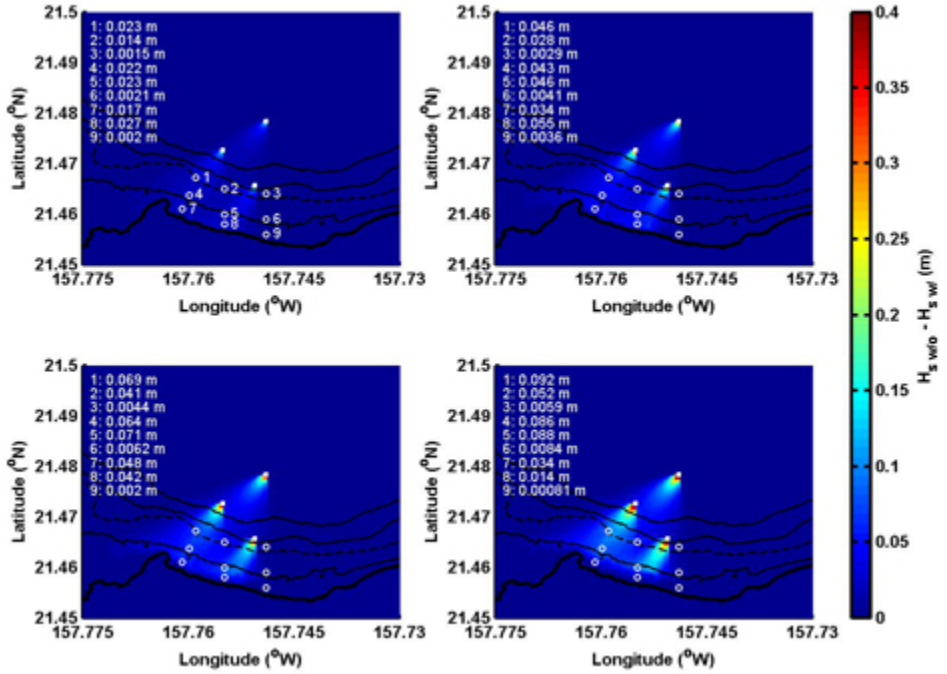

Figure 12. Same caption as Figure 11 but for MWD = 30°.

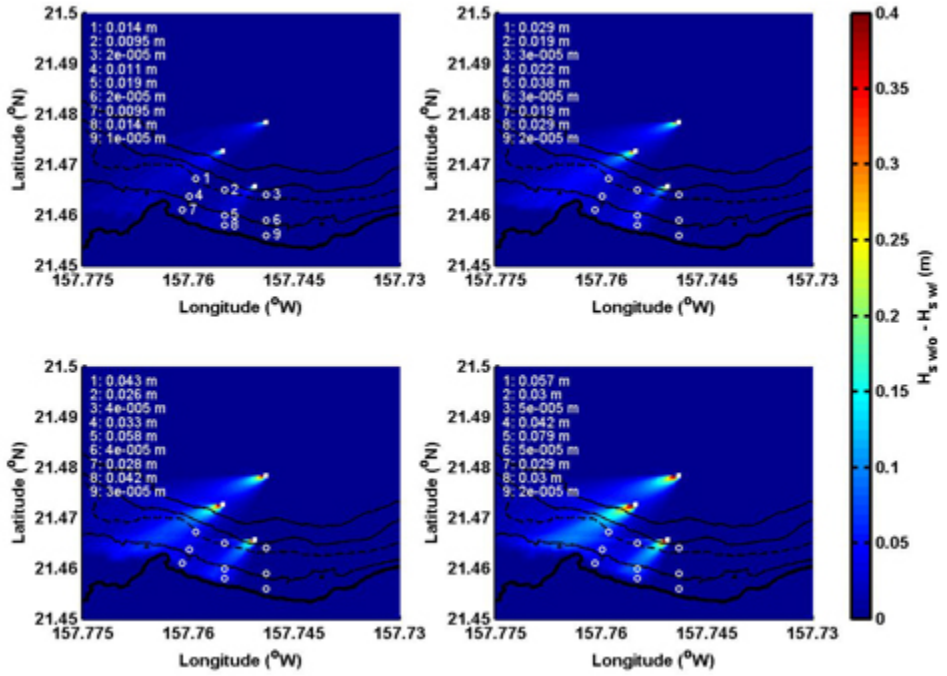

Figure 13. Same caption as Figure 11 but for MWD = 60°.

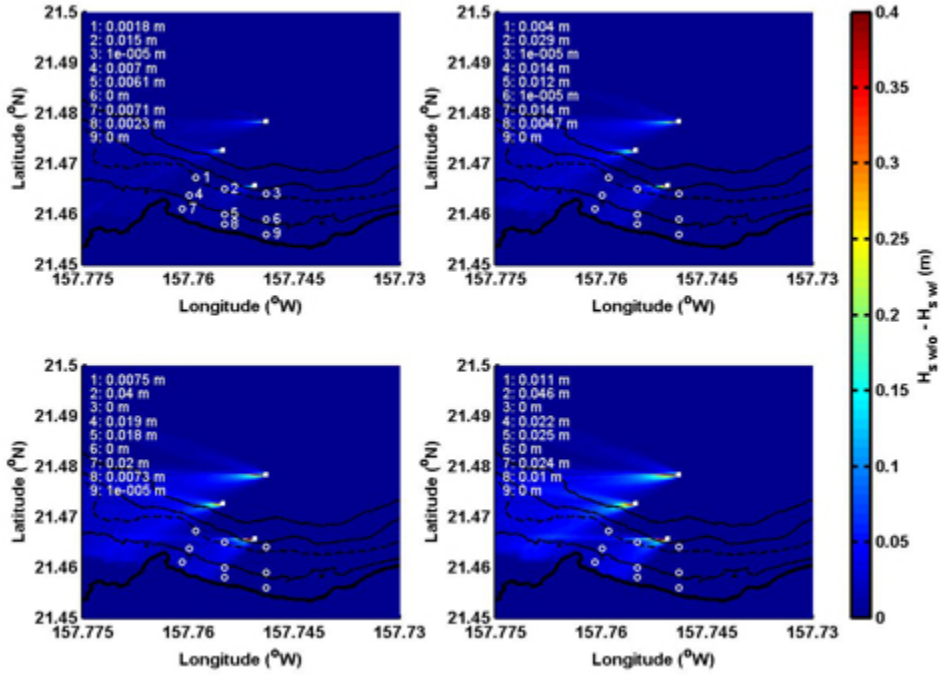

Figure 14. Same caption as Figure 11 but for MWD = 90°.

The effects of WEC devices (i.e. obstacles) on nearshore bottom orbital wave velocities are shown in Table 5 and Figures 15 and 16. Bottom orbital velocity can decrease by greater than 6.5% directly inshore of the obstacle array (location 6) with model initiation parameters: H_s = 4 m, T_p = 10 s, and

MWD = 330°. On average, bottom orbital velocity decreased by 0.007 m/s or 1.4% with the inclusion of obstacles.

Table 5. Statistics of the differences between U_{bot} *with* and *without* obstacles at nine (9) output point locations for 100 nested model runs (model boundary conditions: H_s = 1, 2, 3, and 4 m; T_p = 6, 8, 10, 12, and 14 s, and MWD = 0, 30, 60, 90, and 330°). Values for the 5 m contour, 10 m contour, and 20-25 m contour are also provided.

Output location	Mean		Minimum		Maximum		Standard Deviation	
	%diff	m/s	%diff	m/s	%diff	m/s	%diff	m/s
1	1.12	0.003	0.01	0	2.99	0.018	1.03	0.004
2	2.13	0.005	0.86	0	4.69	0.021	0.96	0.004
3	0.61	0.001	0	0	3.24	0.006	0.85	0.002
4	1.23	0.006	0.02	0	2.57	0.026	0.82	0.006
5	2.07	0.011	0.25	0	3.16	0.031	0.72	0.008
6	1.69	0.007	0	0	6.51	0.037	2.28	0.009
7	1.11	0.007	0.01	0	2.35	0.022	0.74	0.005
8	1.51	0.011	0.05	0	3.10	0.029	0.88	0.007
9	1.26	0.008	0	0	5.90	0.045	1.92	0.012
5 m	1.29	0.008	0	0	5.90	0.045	1.18	0.008
10 m	1.66	0.008	0	0	6.51	0.037	1.27	0.008
20 – 25 m	1.29	0.003	0	0	4.69	0.021	0.95	0.003

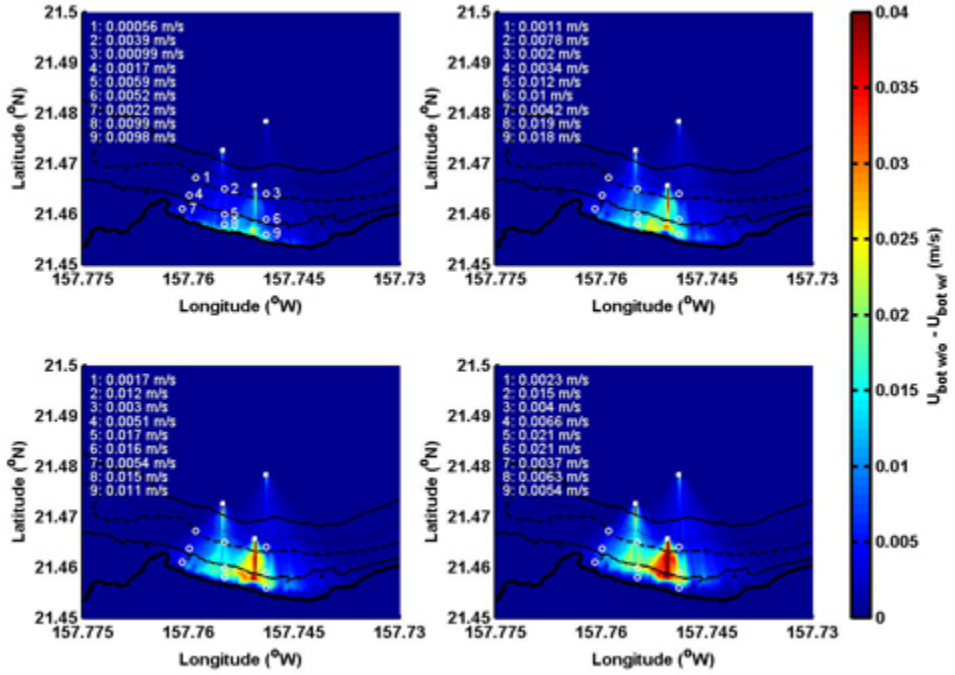

Figure 15. Evaluation of the effects of an obstacle array on the nearshore bottom orbital velocity. The model initiation parameters were: MWD = 0°; T_p = 10 s; and H_s = 1 m (upper left), 2 m (upper right), 3 m (lower left), and 4 m (lower right). The bold line denotes the shoreline and contour lines for 10 m, 20 m, 30 m, and 40 m are shown.

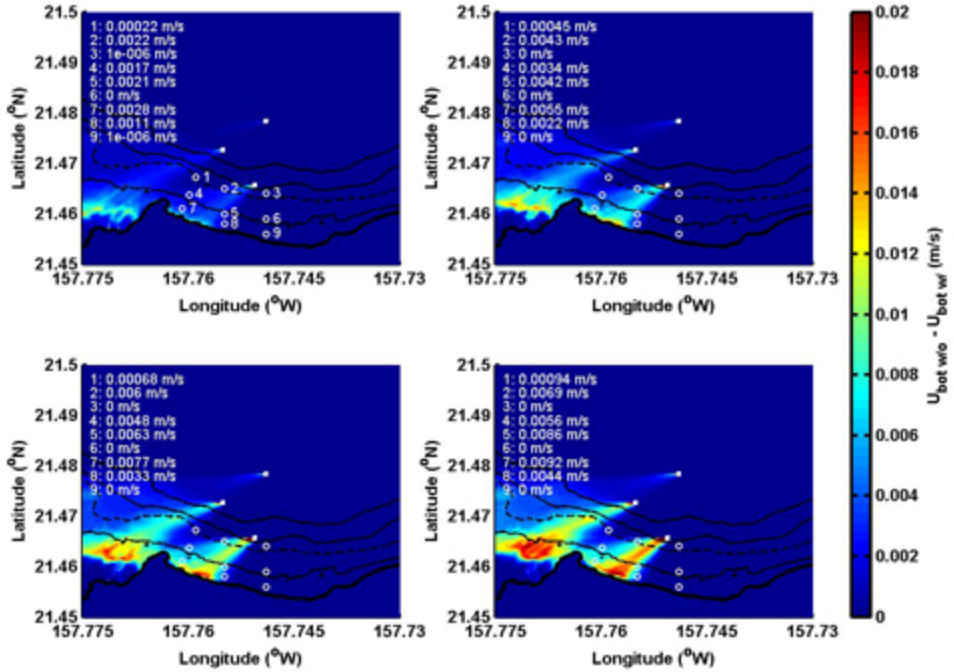

Figure 16. Same caption as Figure 15 but for MWD = 90°.

Summary

The numerical model, SWAN, was used to simulate wave conditions at a potential WETS site in Kaneohe Bay, HI in order to assist with determination of the effects of WEC devices on the propagation of waves into shore. The SWAN model was validated with CDIP buoy wave parameter measurements at Station Mokapu Point. Validation results showed good agreement between modeled and measured significant wave height, peak period, and mean wave direction.

A nested model was evaluated for a range of offshore, deepwater significant wave heights (1 to 4 m), peak periods (6 to 14 s), and mean wave directions (330° to 90°). The impact of WEC devices on the study area was evaluated by simulating an array of three devices within a nested, finer grid SWAN model domain. WEC devices were represented in the model as "obstacles".

Differences between significant wave height in the presence and absence of the WEC device array over the range of specified wave heights, periods, and directions were assessed at nine (9) locations nearshore of the array. The maximum percent decrease in wave height due to the array of three obstacles was predicted to be approximately 6% at 5 m and 10 m water depths (locations 6 and 9). This occurred for model initiation parameters of H_s = 3 m, T_p = 10 s, and MWD = 330° for location 9 (5 m) and H_s = 4 m, T_p = 10 s, and MWD = 330° for location 6 (10 m). Subsequently, bottom orbital velocities were found to decrease by about 6% at the same locations.

It is important to note that this is a very preliminary investigation meant to demonstrate an approach for assessing the effects of WEC devices on near-shore wave fields and the subsequent potential for altering near shore sediment transport. For these initial simulations, WEC devices were assumed to completely absorb the incident wave energy. For environmental purposes this is a very conservative estimate and will lead to the maximum changes (unrealistically large) in wave

propagation parameters. Considering this, the initial simulations show that WEC devices simulated in this way show very minor changes in wave properties near shore. Although final conclusions should not be drawn from this initial study, preliminary indications show that the deployment of three WEC devices at the WETS test site will have negligible impact on near-shore wave climate or shoreline erosion.

References

Komen, G.J., L. Cavaleri, M. Donelan, K. Hasselman, S. Hasselman, and P.A.E.M. Janssen (1994) Dynamics and Modeling of Ocean Waves, Cambridge University Press, New York, 532 pp.